Fusion Engineering and Design 162 (2021) 112079

Contents lists available at ScienceDirect

Fusion Engineering and Design

journal homepage: www.elsevier.com/locate/fusengdes

Performance of a high vacuum, high temperature compatible millimeter-range viewing dump for the vertical ECE experiment on TCV

A. Tema Biwole [a,*], L. Porte [a], A. Fasoli [a], A. Simonetto [b], O. D'Arcangelo [c], the TCV team [1]

[a] Ecole Polytechnique Fédérale de Lausanne (EPFL), Swiss Plasma Center (SPC), CH-1015 Lausanne, Switzerland
[b] CNR Istituto per la Scienza e Tecnologia dei Plasmi (formerly CNR-IFP), via R. Cozzi 53, 20125 Milano, Italy
[c] ENEA Centro Ricerche Frascati (formerly with CNR-IFP), Via Enrico Fermi 45, 00044 Frascati (Roma), Italy

ARTICLE INFO

Keywords:
Tokamak
Electron cyclotron emission (ECE)
Microwaves
Viewing dumps
MACOR

ABSTRACT

A high vacuum and high temperature compatible viewing dump, made of MACOR, was designed and installed in TCV for Vertical ECE experiments in the 75–110 GHz frequency range. Measurements of the dump prior to installation in the tokamak showed in more than 99% of absorption of the incoming radiation. The dump has remained in-vessel more than 7 years, protected from direct plasma exposure by carbon tiles. However it has still been exposed to carbon and boron deposition. Very recently, ex-vessel and in-vessel measurements were carried out over an extended frequency range up to 170 GHz to assess the change in performance of the dump due to exposure in the Tokamak. The new results show that the dump performance has not been adversely affected by seven years of in-vessel exposure and in fact match the original measurements, showing that the dump is still suitable for Vertical ECE experiments on TCV.

1. Introduction

In TCV, the *Tokamak Configuration Variable*, Electron Cyclotron Emission (ECE [1,2]) is used routinely to infer the electron temperature [3]. This is made possible by measuring the emission along a horizontal line of sight from the Low magnetic Field Side of the machine, see Fig. 1. This arrangement known as LFS ECE allows measurements of local electron temperature exploiting the $1/R$ dependence of the emission frequency ($\omega_{ce} \sim 1/\gamma R$), R being the machine major radius and γ the relativistic factor. Under certain conditions, the measured frequency can be unequivocally attributed to a radial location in the plasma, and the temperature at that location can be deduced from the emission intensity. When the conditions change such as when, for example, the plasma electrons depart from a Maxwellian distribution, another ECE arrangement, the Vertical ECE (VECE) [4] can be used to diagnose the properties of the high energy (suprathermal) electrons. The VECE focuses on a sight at constant major radius ($R \approx \text{constant} \Rightarrow \omega_{ce} \sim 1/\gamma$), making it optimal to measure the downshifted (in frequency) emission of suprathermal electrons. VECE measurements, whose aim is measuring suprathermal electron radiation, need the presence of a viewing dump to absorb unwanted thermal radiation. Another way to prevent the contamination of VECE measurements by thermal radiation is to use a retro-reflector instead, which bounces back any incoming wave [5]. The thermal radiation, reflected from the retro-reflector undergoes multiple other reflections in the machine chamber and may ultimately reach the detection system. Viewing dumps have thus been preferred throughout years to retro-reflectors as they drastically reduce multiple reflections of the thermal radiation [6,7]. In this paper, we present the design and performance of a custom-made viewing dump made of MACOR. Of particular interest is the evolution of the dump properties after years of exposure in the high vacuum and high temperature environment of the TCV tokamak. The performance of the dump is characterized in terms of its capacity to absorb electromagnetic radiation in the millimeter range with wavelengths $1.75 < \lambda(\text{mm}) < 4$. The wavelength window corresponds to the frequency range of VECE measurements on TCV ($75 < f(\text{GHz}) < 170$). The absorbing properties of the dump are assessed by measuring its reflectivity both on-axis i.e. the reflection of a wave incident normal to the plane of the dump, and off-axis i.e. the reflection in the normal direction of waves incident with different angles with respect to the normal, as illustrated in Fig. 1. On-axis reflectivity is needed for an accurate estimate of the radiation reaching the VECE antenna facing the dump at the top of the machine. Off-axis reflectivity, on the other hand, is the key parameter to assess the dump capability to prevent stray thermal radiation from entering the detection system. In

* Corresponding author.
E-mail address: arsene.temabiwole@epfl.ch (A. Tema Biwole).
[1] See author list of S. Coda et al. 2019 Nucl. Fusion 59 112023.

https://doi.org/10.1016/j.fusengdes.2020.112079
Received 2 June 2020; Received in revised form 18 October 2020; Accepted 25 October 2020
Available online 9 November 2020

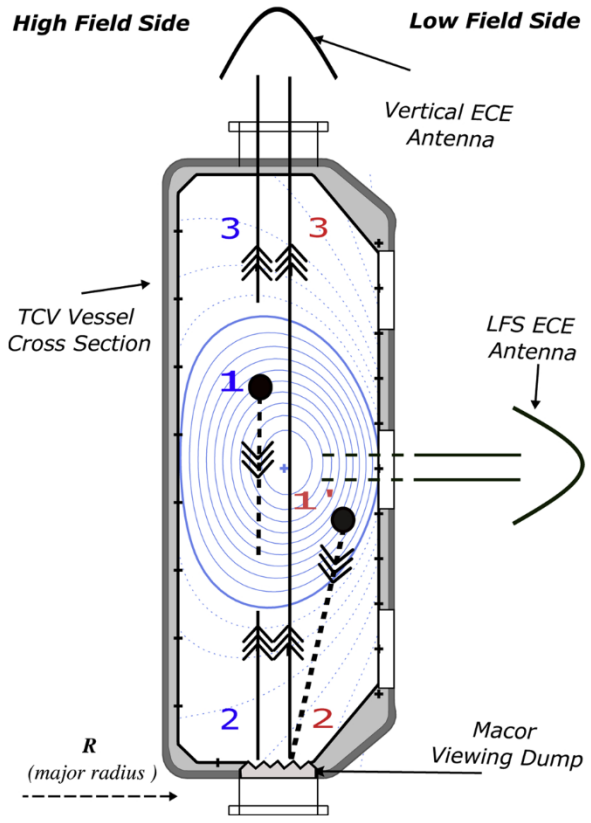

Fig. 1. TCV cross section with a representation of the MACOR viewing dump and the antennas for horizontal and vertical ECE. The radiation reaching the VECE antenna may originate from a region outside the line of sight, in the Low Field Side, following the path 1'-2-3. This is the unwanted thermal radiation for which the assessment of the off-axis reflectivity of the dump is needed. The path 1-2-3 can be taken by both the thermal and the suprathermal radiation within the VECE line of sight.

general, the performance of several dump designs has been very well ascertained and their importance for VECE experiments is now confirmed [8]. The assessment of the dump performance and its degradation due to exposure in the tokamak is the most novel contribution of this paper.

2. Design

A viewing dump for the vertical ECE experiment on TCV must be highly absorbing (> 99% of incoming radiation) and compatible with the high temperature and high vacuum environment of the tokamak. The dump is made out of MACOR, a machinable glass-ceramic.

Glass-ceramics were accidentally discovered by S. Donald Stookey at Corning Inc in the early fifties [9]. Successively, some measurements [10] reported the absorption coefficient of MACOR to vary between $0.08 < \alpha(\mathrm{mm}^{-1}) < 0.15$ (in our frequency range). These values of absorption coefficient increase with frequency and are at least one order of magnitude higher than the values for common low loss ceramics. In appearance, MACOR is a white, porcelain-like material composed of 46% Silicon – SiO_2, 17% Magnesium – MgO, 16% Aluminum – Al_2O_3, 10% Potassium – K_2O, 7% Boron – B_2O_3 and 4% Fluorine – F, see [11]. MACOR has a continuous operating temperature of 800 °C and a peak temperature of 1000 °C. It is easily machinable and can be considered to withstand high heat fluxes. It does not outgas in vacuum environments. It is strong, non-porous, radiation resistant and therefore a good candidate for a viewing dump in a plasma confinement device.

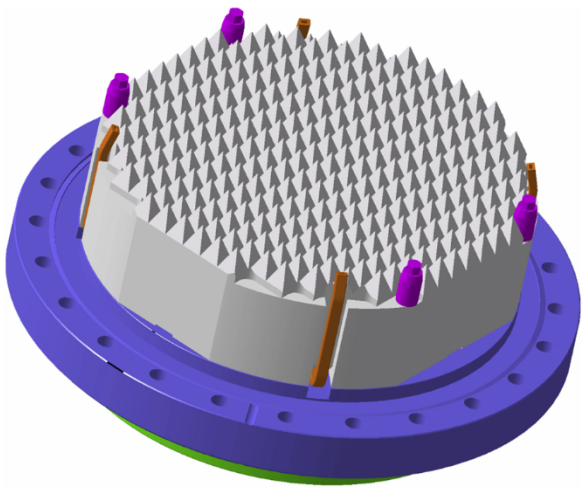

Fig. 2. TCV viewing dump design: array of pyramids with 90° rotational symmetry.

The preferred viewing dump shapes are straight grooves, array of horns or pyramid arrays. Those shapes increase the absorption of the incident wave by geometric means inducing multiple reflections. Straight grooves are the easiest to fabricate but the absorption is strongly dependent of the relative orientation of the dump. In fact, dumps featuring straight grooves exhibit high reflectivity for wave polarization parallel to the grooves. The TCV dump (Fig. 2) is an array of pyramid ($10 \times 10 \times \sim 11.6$ mm), which is difficult to manufacture but does not have a preferential orientation. The angle between faces of adjacent pyramids is 45° (see Fig. 3) resulting in at least 4 reflections of the wave in the MACOR, thus greatly enhancing absorption.

Spatial constraints on TCV limit the size of the dump to a maximum diameter of ~200 mm (Fig. 4). This number will end up to be very important for the application of the dump, as it can be sometimes smaller than the beam size at the dump location due to refraction effects. The size of the pyramids was chosen based on the optical thickness of MACOR in this frequency range, approx. 10 mm.

3. Performance

The performance of the TCV dump is evaluated measuring its reflectivity in the proper frequency range. This was done prior to the installation of the dump in the TCV tokamak and has now been repeated 12 years later.

3.1. Before the exposition to the plasma in the TCV tokamak

The dump was measured at CNR-IFP (now CNR-ISTP) Milano in 2007 prior to installation in TCV [12]. Measurements were made with an AB Millimetre 8-350 Vector Network Analyzer equipped with WR-10 heads. Transmittivity, on- and off-axis reflectivity were measured with rows of pyramids parallel and at 45° to incident polarization. Off-axis reflectivity was also measured for polarizations parallel and perpendicular to the plane of incidence. Measurements were made using antennas directly viewing the dump, their distance chosen for minimizing sensitivity to individual pyramids and to dump edge effects. On- and off-axis reflectivities were always lower than approx − 25 and − 35 dB

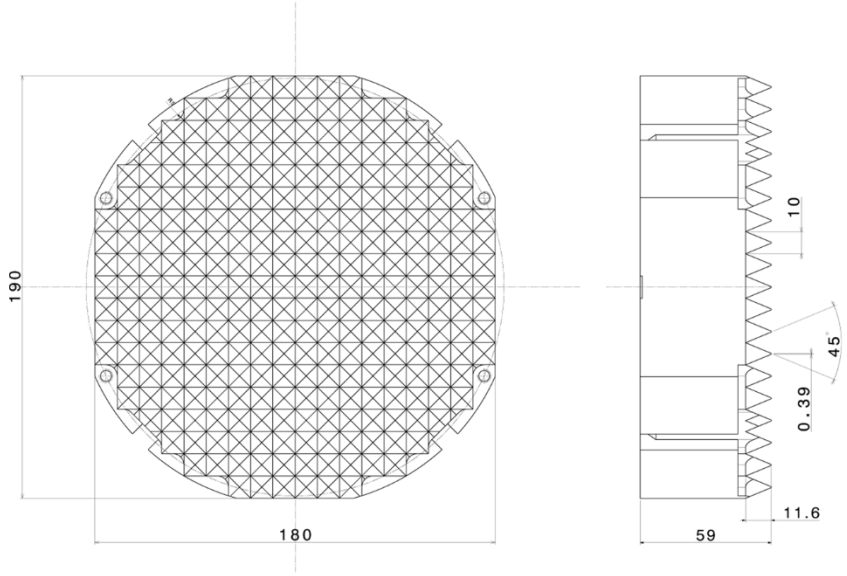

Fig. 3. Drawing of TCV viewing dump showing detailed design parameters.

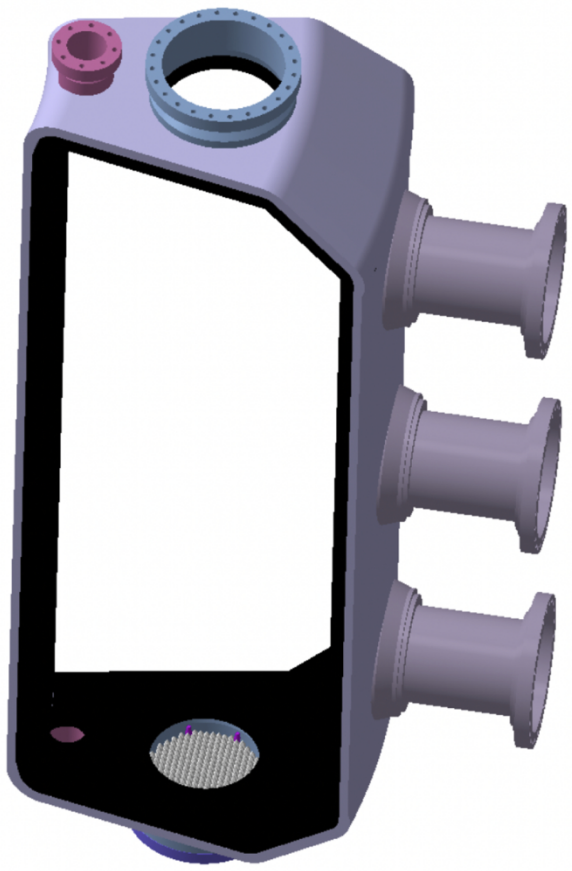

Fig. 4. Viewing dump fit within a TCV port.

respectively. On-axis reflectivity measurements were limited by noise and incomplete removal of systematics due to the poor match of the antennas available at the time, so the results should be viewed as an upper limit.

3.2. After several years in the TCV tokamak

The original dump measured in Section 3.1 was damaged and replaced by an identical copy in 2012. It was damaged by high microwave power (~500 kW) from the plasma heating system. The damage is probably the result of the high absorption coefficient, low thermal conductivity and low toughness of the MACOR, coupled with a mishap in the orientation of the microwave antenna. During routine operation though, the dump is irradiated without risk by the plasma itself, receiving microwave power $\lesssim 10^{-4}$ W. What is first discussed in this section is the effect on the dump of the direct heat and particle flux from the scrape off layer plasma in TCV, i.e. the plasma outside the last closed flux surface (LCFS).

The dump has been present in the machine for about seven years and has witnessed ~17,580 plasma discharges. Not all plasmas could have potentially affected the dump directly. The discharges in the so-called limited configuration (Fig. 5a) allow only minimal interaction between the plasma and the dump. The interaction can lead to relevant particles and heat deposition on the dump only in diverted configurations such as the one represented in Fig. 5, with the divertor leg at the radial position of the dump. In that case the exposure of the dump to the plasma also depends on the angle of incidence of the grazing magnetic field lines. A minimum angle of incidence of 13° would be necessary for direct heat deposition along the magnetic field lines. This value is unpracticable on TCV. In fact, the combination of the magnetic field generated by the plasma current and the one externally generated from poloidal and toroidal coils leads to field lines with an incident angle on the dump of at most ~8°. In this worst case scenario, the power in the order of a few MW/m^2, is deposited at ~17 mm above the dump pyramids, see Fig. 6.

As a conclusion, it is clear that the TCV dump never faced direct heat and particle deposition from the plasma, explaining its integrity. What has changed is the color of the front face of the dump which departed from the initial white color of the ceramic due to some carbon deposition. The carbon deposition observed on the dump and pictured in Fig. 7 may have originated from cross-field transport of carbon ions, sputtered

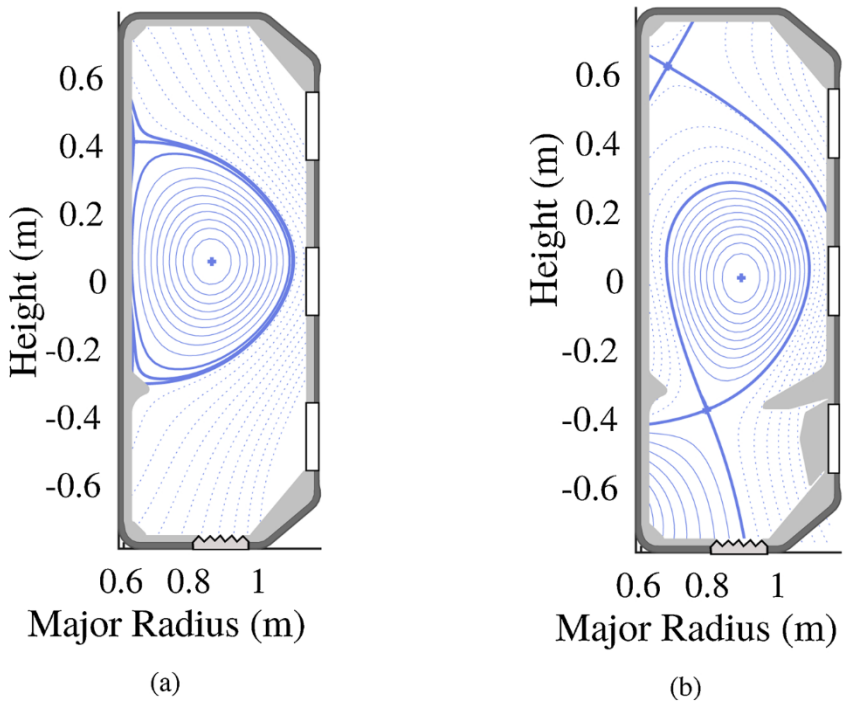

Fig. 5. Example of plasma discharges in a limited configuration (a) and in a diverted configuration with divertor leg on the dump (b). Both configurations are ohmically heated Low confinement-mode discharges. LCFS and divertor legs are represented in bold lines.

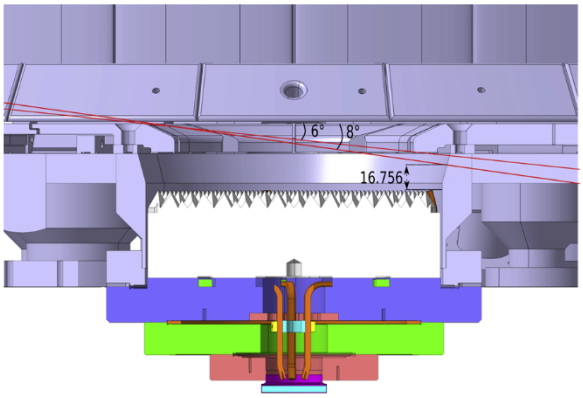

Fig. 6. The dump pyramids are 45 mm below the floor, with an incidence angle of 8° which is a limit value on TCV, the heat and particles are deposited ~16.7 mm above the dump pyramids.

from graphite tiles in the machine and then travelling mostly along the magnetic field lines. Another process for carbon deposition, although less important (deposited material will be much thinner), is the deposition of carbon from the neutral carbon atoms and neutral carbon molecules [13]. These electrically neutral particles can be deposited even in region hidden from the direct exposure to the magnetic field lines. The presence of the carbon coating on the dump, following its exposition in the Tokamak (Fig. 8), could have altered its properties; this is the motivation of the following measurements.

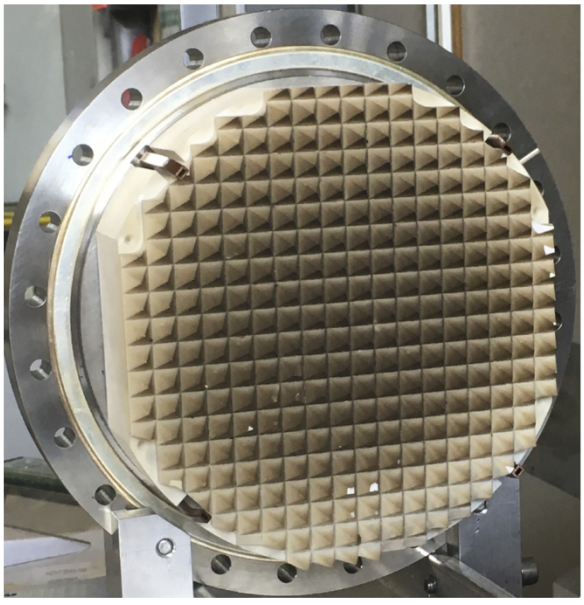

Fig. 7. Preferential carbon deposition (more deposition on the top, less in the bottom on the right-hand-side figure) tells that TCV experiments are more frequently performed with a specific helicity.

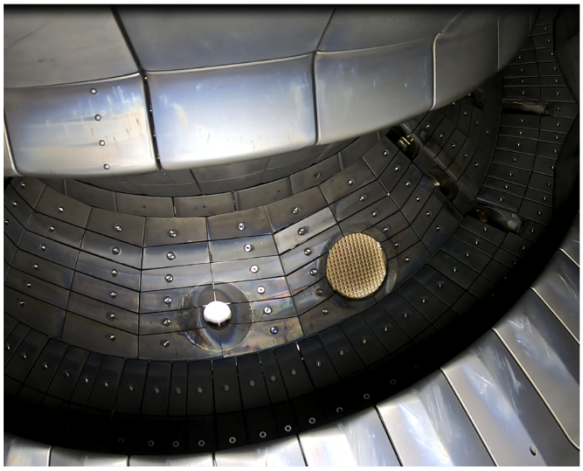

Fig. 8. Viewing dump exposed to heat and particle flux in the TCV vessel.

3.2.1. Measurement of the dump reflectivity, removed from the machine

The dump reflectivity was first measured, while removed from the machine, with two different optical setups. Both setups used a Keysight Vector Network Analyzer (VNA) of type PNA N5224A 10 MHz to 43.5 GHz. The native frequency range of the VNA was extended above the 43.5 GHz limit using modules of Virginia Diodes Inc (VDI) extension heads. The heads included a transceiver/receiver module (TX/RX) and a only receiver module (RX). The on-axis reflectivity of the dump was readily measured with the TX/RX module in reflectometry mode, while the off-axis reflectivity was measured using both modules with the RX modules fixed on axis, and the TX/RX modules scanning different angles around the normal direction.

One of the optical setups included the use of horn antennas for measurements in the frequency range 70–110 GHz, see Fig. 9a. For the on-axis reflectivity, a smooth-walled circular horn of aperture ∼16.3 mm was attached to the TX/RX module, thus producing a beam of diameter ∼12.3 mm at the antenna aperture. A Teflon lens (index of refraction ∼1.4 [14]) was positioned at ∼150 mm from the horn, obtaining a beam waist of ∼49 mm for a wave at 70 GHz (focal length at ∼430 mm from the lens) and a beam waist of ∼30 mm for a wave at 110 GHz (focal length at ∼270 mm from the lens). The beam size was computed using Gaussian beam optics [14]. The computed beam diameter at the dump (situated at ∼1 m from the lens, see Fig. 9b) varied with frequency between ∼80 mm at 70 GHz and ∼86 mm at 110 GHz. Stray environmental reflections were suppressed with Eccosorb as absorbing material. The pieces of Eccosorb are not shown in the figure, they were put all around the antenna. An attempt was made to measure off-axis reflectivity, this time keeping the receiver in front of the dump and moving the transceiver, a picture is in Fig. 10. It was much difficult in this case to focus the beam and the resulting values of reflectivity were much lower than the ones measured on-axis and shown in Fig. 11.

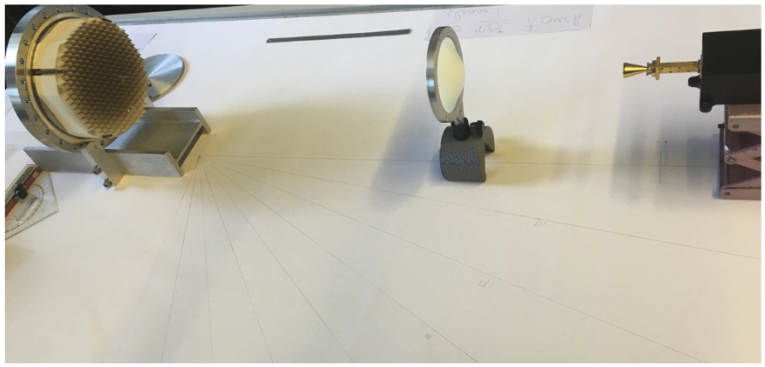

(a)

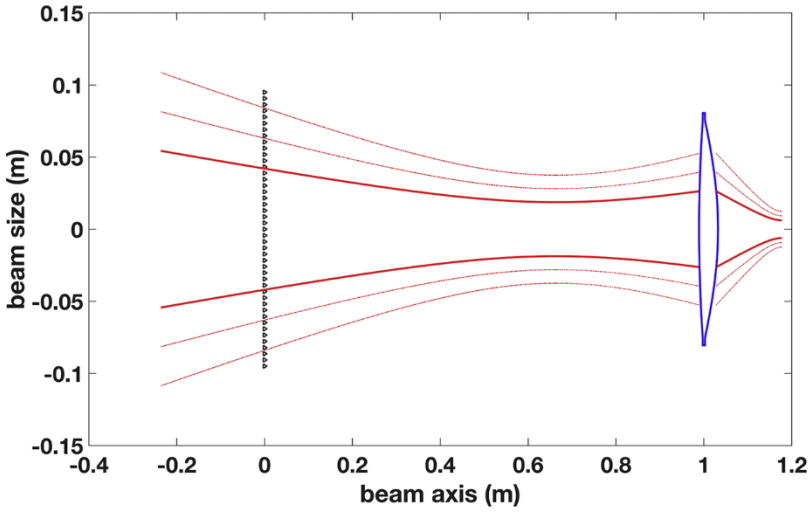

(b)

Fig. 9. Experimental setup for dump on-axis reflectivity measurement with horn antenna and focusing Teflon lens (a). The pattern of a 90 GHz beam has been computed using Gaussian beam optics applied to our experimental setup (b). The bold line corresponds to the beam size at which the field amplitude falls to $1/e$ relative to its on-axis value, ω ($1/e$ power width). The dashed lines corresponds respectively to 1.5ω (98% power width) and 2ω (99.97% power width.)

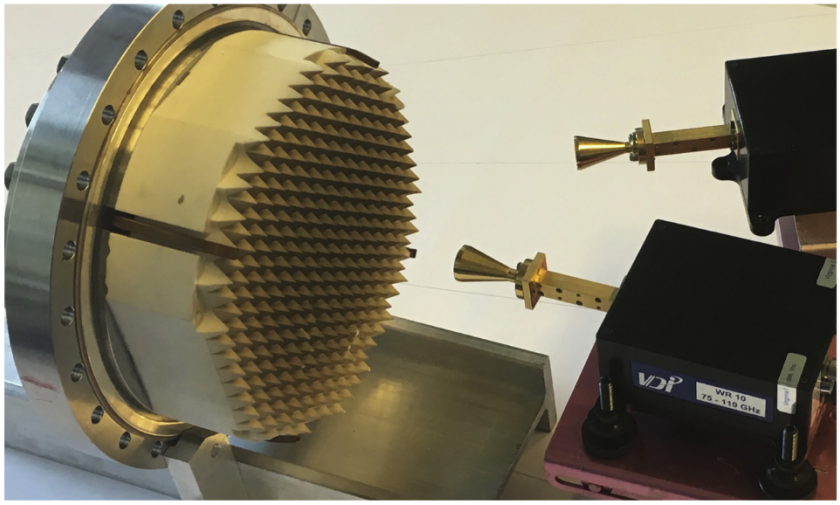

Fig. 10. Example of setup for off-axis reflectivity.

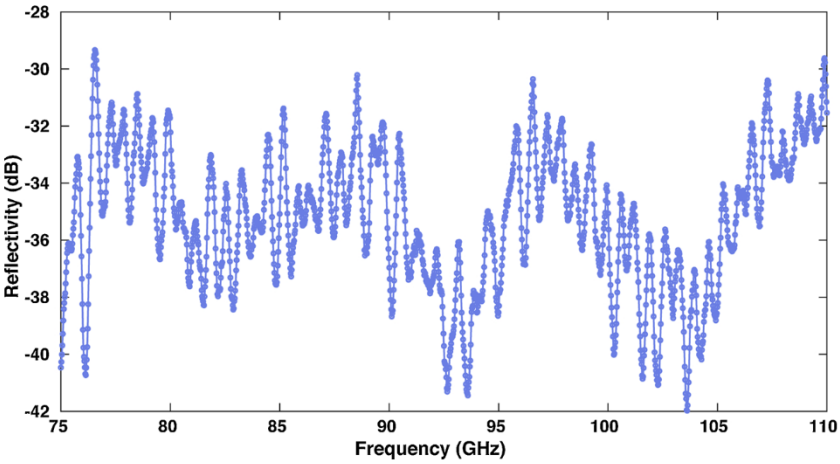

Fig. 11. Result of dump on-axis reflectivity measurement.

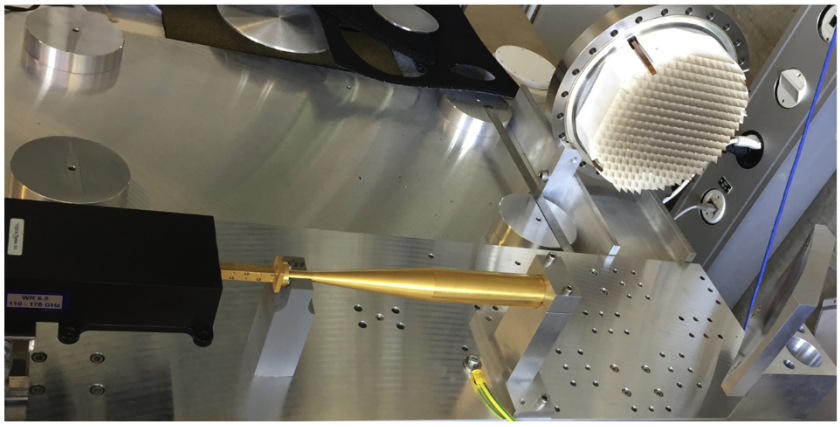

Fig. 12. Optical table configuration for only S11 measurement.

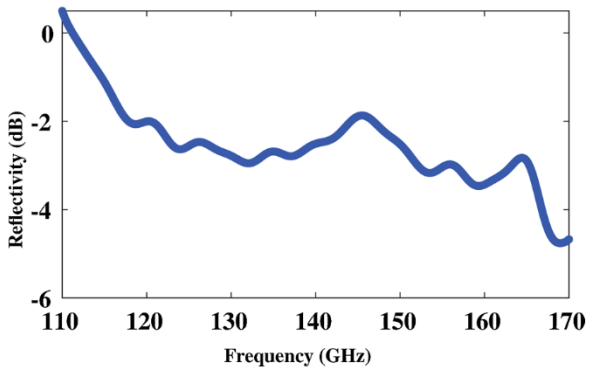

Fig. 13. Measurement of the reflectivity of the Aluminium plate.

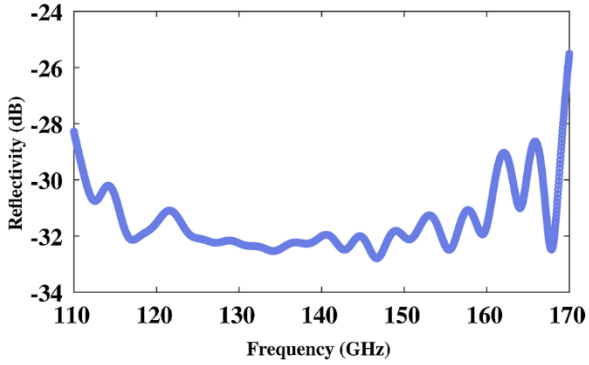

Fig. 14. Result of dump reflectivity on optical table.

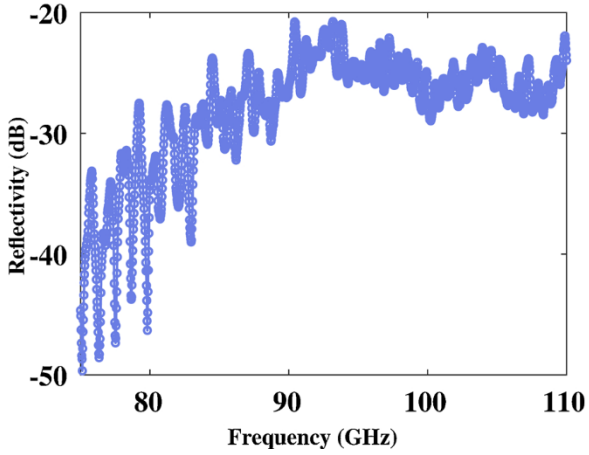

Fig. 15. Result of dump S11 measurement on TCV site. Higher values come from the frame of the dump, as the beam pattern did miss the dump in part.

Another measurement of the dump was performed on the free-space quasioptical table pictured in Fig. 12 in the frequency range 110–170 GHz. The table is equipped with corrugated horn antennas in the WR-6.5 and WR-4 bands which produce axially symmetric beams with low side lobes. The focus of the table allows samples of ~100 mm diameter to be measured. For the reflectivity measurement of the dump, the instrument was calibrated using as perfect reflector, an Aluminium plate whose S11 parameter is shown in Fig. 13 (S11 defines the reflectivity, the term 11 of the scattering matrix). All the measurements presented in this work used the same plate for the S11 normalization. The result of dump reflectivity on optical table is shown in Fig. 14.

3.2.2. *Measurement of the dump reflectivity while in the machine*

The objective of this last measurement was to check the reflectivity of the dump as seen by the VECE diagnostic. This measurement is important mostly to check the alignment between the dump and the VECE receiving antenna, which is crucial for the application of the dump. While more will be discussed about the dump application in TCV elsewhere, in this section we focus on the measurement itself. The measurement took place with the dump installed at its location at the bottom of the machine (~1.5 m from the top) and using the optical setup of the VECE. The VECE optics on TCV produces at the dump location, beams of radius ~36 mm at 110 GHz and ~46.4 mm at 70 GHz. Multiple reflections occurred along the path from the VNA to the dump, complicating the measurement. One reflection certainly occurred at the window through which the VECE observes the plasma. Other reflections originated in the waveguides and other metallic spots around the window and the dump. To remove the pervasive reflections shadowing the dump reflectivity, the plate of Aluminium was installed to cover the dump and, by time of flight we isolated the reflection arising exactly at the position of the plate (time gating). We used that value for the calibration and then removed the plate of Aluminium and repeated the process with the dump instead.

The result for this measurement is shown in Fig. 15. The reflectivity at the lower frequencies is unexpectedly low compared to the one at higher frequencies. It can be that the radiation at low frequencies are diffused in the machine chamber and do not reach back the antenna. The bigger radiation pattern at lower frequencies could explain the significant loss of signal. This hypothesis cannot be confirmed on the basis of what has been done in this work, but what is interesting in the result are the values at higher frequencies which set the upper limit of the reflectivity as seen by the VECE. In fact, values of reflectivity at higher frequencies, which come close to − 20 dB include also the reflection at the metallic frame around the dump. Situations where the VECE beam pattern intersects the frame around the dump are common during TCV operation, the frame around the dump was previously shown in Fig. 8.

4. Conclusion

The measurement of the dump prior to installation in TCV [12] resulted in an average (over frequencies) of off-axis reflectivity below − 35 dB (see Fig. 16). The average value for on-axis reflectivity was around − 30 dB. The dump on-axis reflectivity measured in 2019 after years in the tokamak resulted in average value around − 31 dB in the 110–170 GHz range (Fig. 14), and around − 35 dB in the 70–110 GHz range.

It is important to mention that both measurements were made using a simple correction of the response, instead of a free-space VNA calibration including all the discontinuities up to the antenna (see e.g. [15–17]). Therefore, both measurements overestimate the dump reflectivity. Nonetheless, the new measurement is fully compatible with the old one, see Fig. 17, which shows beyond doubt that the dump performance was not affected by the plasma within the sensitivity margins of the measurements. Thus, the reflectivity of the TCV viewing dump was not altered after years in the machine and lies below a value of − 30 dB. In practice, a reflectivity of around − 30 dB means that the dump reflects ~0.1% (or alternatively that it absorbs ~99.9%) of the incident power. Therefore, the dump performance still fulfills the requirements for VECE experiments on TCV.

Declaration of Competing Interest

The authors report no declarations of interest.

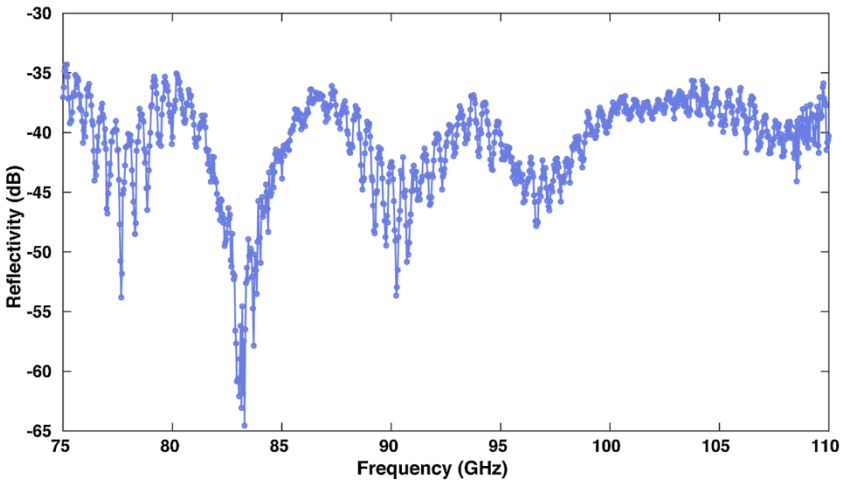

Fig. 16. A result of off-axis reflectivity of the dump as measured in 2007 with the TX/RX module at 30° from the axis of the dump.

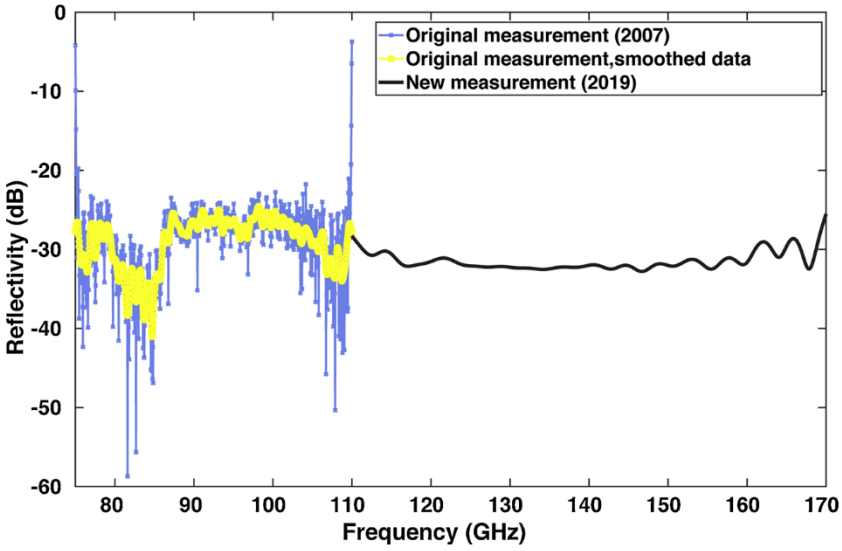

Fig. 17. Comparison of the measured reflectivity, the S11 parameter, before exposition in the tokamak (original measurement in 2007) and after years of exposition (new measurement 2019).

Acknowledgments

The authors would like to thank Stefano Coda for reviewing this work and for providing great insights on the topic. Hugo De Oliveira and Christian Theiler are gratefully acknowledged for the helpful discussions on the heat and particles deposition on the dump. This work has been carried out within the framework of the EUROfusion Consortium and has received funding from the Euratom research and training programme 2014–2018 and 2019–2020 under grant agreement No 633053. The views and opinions expressed herein do not necessarily reflect those of the European Commission. This work was supported in part by the Swiss National Science Foundation.

References

[1] H.J. Hartfuss, T. Geist, Fusion Plasma Diagnostics with mm-Waves, chapter IV: Passive Diagnostics, 2013, pp. 117–150.
[2] M. Bornatici, R. Cano, O. De Barbieri, F. Engelmann, Electron cyclotron emission and absorption in fusion plasmas, Nucl. Fusion 23 (9 (sep)) (1983) 1153–1257.
[3] V.S. Udintsev, G. Turri, E. Asp, C. Schlatter, T. Goodman, O. Sauter, H. Weisen, P. Blanchard, S. Coda, B. Duval, E. Fable, A. Gudozhnik, P. Isoz, M.A. Henderson, I. Klimanov, X. Llobet, P. Marmillod, A. Mueck, L. Porte, H. Shidara, Recent electron cyclotron emission results on TCV, Fusion Sci. Technol. 52 (2007) 08.
[4] L. Porte, S. Coda, S. Alberti, R. Bertizzolo, R. Chavan, J. Mayor, A. Simonetto, V. S. Udintsev, A Vertical ECE Diagnostic for TCV, 2007.
[5] R. James, S. Janz, R. Ellis, D. Boyd, J. Lohr, Vertical-viewing electron cyclotron emission diagnostic for the DIII-D tokamak, Rev. Sci. Instr. 59 (1988) 1611.
[6] K. Kato, I.H. Hutchinson, Diagnosis of mildly relativistic electron velocity distributions by electron cyclotron emission in the Alcator C tokamak, Phys. Fluids 30 (1987) 3809.
[7] T. Luce, P.C. Efthimion, N.J. Fisch, R.E. Bell, J.E. Stevens, Modelling of vertical ECE during lower hybrid current drive on PLT, AIP Conf. Proc. 159 (1987) 167.
[8] K. Kato, I.H. Hutchinson, Design and performance of compact vacuum-compatible submillimeter viewing dumps, Rev. Sci. Instr. 57 (1986) 1242.
[9] J.M.F. Haussonne, C. Carry, P. Bowen, J.L. Barton, Céramiques et verres: principes et techniques d'élaboration, Traité Matériaux 16 (2005) 830.
[10] M.N. Afsar, K.J. Button, Precise millimeter-wave measurements of complex refractive index, complex dielectric permittivity and loss tangent of GaAs, Si, SiO2, Al203, Beo, Macor, and Glass, IEEE Trans. Microwave Theory Tech. 31 (1983) 217–223.
[11] Corning, MACOR Machinable Glass Ceramic For Industrial Applications, 2012.
[12] O. D'Arcangelo, A. Simonetto, S. Garavaglia, V. Muzzini, Internal report FP07/03 CNR: Performance of a macor beam dump for Vertical ECE diagnostic by EPFL Lausanne in the 75–110 GHz band, Consiglio nazionale delle ricerche, Istituto di Fisica del Plasma, Via Cozzi 53, 20215 Milano, Italy, May (2007).
[13] J.P. Coad, D.E. Hole, M. Rubel, A. Widdowson, J. Vince, Deposition results from rotating collector diagnostics in JET, Phys. Scr. T138 (2009) 014023.
[14] P. Goldsmith, Quasioptical Systems – Gaussian Beam Quasioptical Propagation and Applications, IEEE Press, 1998, p. 01.
[15] I. Rolfes, B. Schiek, Calibration methods for microwave free space measurements, Adv. Radio Sci. Kleinheubacher Berichte 2 (2004) 01.
[16] A. Murk, A. Duric, F. Patt, Characterization of ALMA calibration targets, 19th International Symposium on Space Terahertz Technology, Groningen (NL), April (2008).
[17] A. Murk, A. Duric, ALMA Calibration Device Prototype Calibration Load Test Report FEND-40.06.04.00-005-A-REP. Technical report, July 2007.